Prediction of solid–binder affinity in dry and aqueous systems: Work of adhesion approach vs. ideal tensile strength approach

Ahmed Jarray, Vincent Gerbaud, Mehrdji Hemati

http://dx.doi.org/10.1016/j.powtec.2014.11.004

Prediction of solid–binder affinity in dry and aqueous systems: Work of adhesion approach vs. ideal tensile strength approach

Ahmed Jarray *, Vincent Gerbaud, Mehrdji Hémati

Université de Toulouse, INP, UPS, LGC (Laboratoire de Génie Chimique), 4 allée Emile Monso, F-31432 Toulouse Cedex 04, France
LGC, INP, ENSIACET, 4 Allée Emile Monso, 31432 Toulouse, France

Keywords:
Agglomeration
Pharmaceutical products
Solubility parameter
Work of adhesion
Tensile strength
Coating

A B S T R A C T

Wet granulation process requires the addition of a coating agent or binder, typically composed of surfactants such as hydroxypropyl-methylcellulose (HPMC), water and a small amount of filler such as stearic acid (SA). In dry granulation however, the coating agent is added to the system in the form of fine solid particles. In both cases, a successful granulation requires good affinity between host and guest particles. In this study, we compare two approaches to predict the binder–substrate affinity in dry and in aqueous media, one based on the work of adhesion and the other based on the ideal tensile strength (Rowe, 1988). The novelties of this paper are four folds. First, the equations used in both approaches are generalized and rewritten as a function of the Hildebrand solubility parameter δ. δ is obtained from molecular simulations or predicted from HSPiP group contribution method. Secondly, a correlation between δ and the experimental surface tension γ is established for cellulose derivative (such as HPMC and ethyl cellulose). Thirdly, the concept of ideal tensile strength, originally formalized by Gardon (1967) for binary systems, is extended to ternary systems and applied for granulation in aqueous media. Fourthly, the approaches are tested for various systems and compared to experimental observations. For dry binary systems, predicted adhesive and cohesive properties agree with literature experimental observations, but the work of adhesion approach performs better than the ideal tensile strength approach. Both approaches predict that HPMC is a good binder for microcrystalline cellulose (MCC). The results also indicate that polyethylene glycol 400 (PEG400) has a good affinity with HPMC and stearic acid. For ternary aqueous systems, the results fully agree with the observations of Laboulfie et al. (2013).

1. Introduction

Granulation is a size-enlargement process during which small particles are formed into larger and physically strong agglomerates [1]. In wet granulation processes (Fig. 1), this is performed by spraying a liquid binder onto the particles as they are agitated in tumbling drum, fluidized bed, high shear mixer or similar device [2,3].

Coating is a process which allows to deposit on the surface of particles a thin film layer which can be of different nature: polymers, salts, sugars, etc. (Fig. 1).

These two operations confer on powder's new properties for customers, such as hydrophobicity, masking bitterness, reducing the risks of explosion, avoiding the segregation of the constituents, improving the flow properties and the compression characteristics of the mix.

Processes of size enlargement involve the coupling of two classes of parameters. The first class corresponds to the local physico-chemical parameters dependent on the nature of the solutions and powders. The second class corresponds to the parameters of the processes which are the constraints exercised by the process equipment on the bed of powder, such as the temperature and the flow rates. The quality of the end product depends on the control of the coupling between these two families of parameters which exist in different scales. At present, the optimization of these parameters, notably the choice of solvent and binders is based on an empirical, by nature long and expensive approach.

The three principal mechanisms of wet granulation are as follows: wetting and nucleation; consolidation and growth; and attrition and breakage [4]. Inspired by Ennis' work [5,6], Benali et al. [7] proposed the modified capillary number Ca' to evaluate the importance of the viscous force with respect to the adhesion work. When the $Ca' > 1$, the cohesion of dynamic liquid bridges during nucleation and growth becomes greater than that of the static liquid bridges. This is attributed to the effect of viscous energy dissipation. When the $Ca' < 1$, the effect of the adhesion force is dominant.

Mastering granule processing under the $Ca' > 1$ regime is routine for laboratory and industrial practitioners. Mastering the $Ca' < 1$ regime

* Corresponding author. Tel.: +33 06 48 45 57 31.
E-mail addresses: ahmed.jarray@ensiacet.fr (A. Jarray), vincent.gerbaud@ensiacet.fr (V. Gerbaud), mehrdji.hemati@ensiacet.fr (M. Hémati).

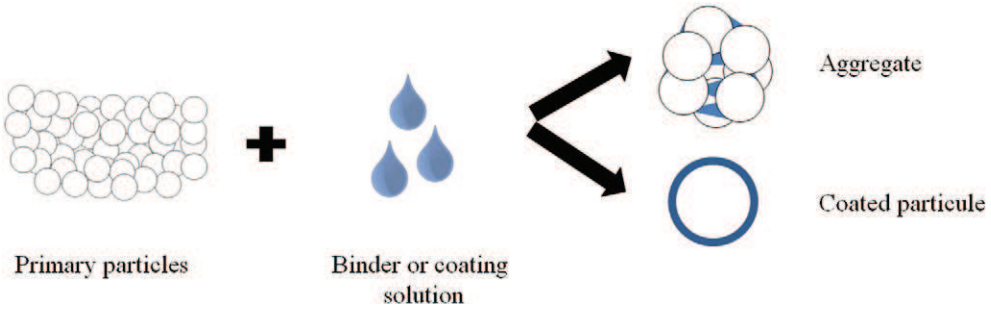

Fig. 1. Wet particle growth mechanisms.

requires to select binders adequately. Formulating the optimum binder or coating is essential even if suitable operating conditions may bring enough mechanical energy to obtain rigid granules.

This work has for objective to develop predictive methodologies and theoretical tools of investigation allowing to choose the adequate binder or to formulate the right coating solution to assure the customer's requested properties of the end product. As such, we explore two theoretical approaches for predicting substrate–binder interactions, one based on the work of adhesion, and the other based on the ideal tensile strength. We extend the approaches to ternary systems so as to study the interactions between compounds mixed in a solvent such as hydroxypropyl-methylcellulose (HPMC) and stearic acid (SA) mixed in water. The background section gives an overview of binders and coatings commonly used in granulation processes. It also reviews some theoretical models for binary mixtures. Then, we derive the tensile strength model for ternary mixtures. The last section concerns the model testing. First, we discuss the selection of the model core data, either coming from group contribution method or from molecular simulations, and we compare them with experimental data. Second, a relationship between the surface free energy and solubility parameter is proposed for cellulose derivatives. Third, it is used next for the prediction of the interactions in binary and ternary mixtures. The predictions obtained through the tensile strength approach and the work of adhesion approach are compared and discussed.

2. Background

2.1. Binder and coating compounds

Cellulose derivatives such as hydroxypropyl methylcellulose (HPMC) and microcrystalline cellulose (MCC) are often used in granulation processes. Generally, HPMC is used as a protective colloid by coating hydrophobic particles with multimolecular layer and promote wetting [8]. MCC is frequently used in pharmaceuticals as a binder/diluent in oral tablet and capsule formulations [9]. Fatty acids such as stearic acid (SA) are often added to the cellulose derivatives to enhance specific properties. For example, adding SA to HPMC leads to a decrease in the water affinity due to SA hydrophobic properties caused by its content of long-chains [10]. Stearic acid is also widely used in oral formulations as a tablet and capsule lubricant [11]. Another additive is the polyethylene glycol (PEG), which can be used in various polymerization grades. Their main advantage over fatty acids is their physical and thermal stability on storage. However, they are chemically more reactive than fats [12] and have only limited binding action when used alone. PEG are often used as plasticizers [13] or added to pharmaceutical mixtures to improve their mechanical properties [14].

2.2. Theoretical models and equations

In order to predict the affinity between the different compounds, we need to calculate the work of adhesion and the ideal tensile strength. These quantities can be obtained using the Hildebrand [15] solubility parameter δ which can be estimated by experimental methods or by using molecular simulation.

2.2.1. Hildebrand solubility parameter δ

As Barton [16] asserted in his handbook of solubility parameters, many properties of polymers can be related to the Hildebrand solubility parameter δ which is proportional to the square root of the cohesive energy density e_{coh}. This parameter describes the intra- and intermolecular forces of a substance. It can also be expressed in terms of the individual Hildebrand parameters describing two contributions to the cohesive energy, namely, the non-polar Van der Waals dispersion forces δ_d, and the polar interactions (electrostatic) δ_p. Hydrogen bonding interactions δ_h are included here in the polar contribution:

$$\delta = \sqrt{\delta_d + \delta_p}. \tag{1}$$

Experimentally, there are numerous methods for Hildebrand solubility parameter determination such as the homomorph method [16], the maximum-in-swelling method often used for the determination of solubility parameters of crosslinked polymers [17], and inverse gas chromatography [18]. Many scientists including Hansen [19], Van Krevelen [20], Hoy [21] and Small [22] and recently Yamamoto (HSPiP [23]) have proposed correlations and lists of contributions for various chemical groups.

In molecular simulation, the Hildebrand solubility parameter can be calculated from the pair potential by summing the pairwise interactions [24]. The cohesive energy density is equal to minus the intermolecular energy, i.e. the intramolecular energy minus the total energy:

$$\delta_k^2 = \frac{<\sum_{i=1}^{n} E_i^k - E_c^k>}{N_{av} <V_{cell}>}. \tag{2}$$

With n the number of molecules in the simulation cell, N_{av} the Avogadro number, and $k = 1, 2$, are the van der Waals energy (dispersion) and the coulombian energy (polar) respectively. "< >" denotes a time average over the duration of the dynamics in the canonical ensemble NVT, V_{cell} the cell volume, the index "i" refers to the intramolecular energy of the molecule i, and the index "c" represents the total energy of the cell. Calculation of the Hildebrand solubility parameter will permit us to estimate the work of adhesion and the ideal tensile strength.

2.2.2. The work of adhesion and cohesion

The energy required to separate unit areas of two surfaces A and B from contact is referred to as the work of adhesion (W_{AB}), and for surfaces of the same material, this is called the work of cohesion (W_{AA}). Girifalco and Good [25] have expressed the work of adhesion in terms of the surface free energy of the pure phases by:

$$W_{AB} = 2\phi_I \phi_V (\gamma_A \gamma_B)^{1/2}. \tag{3}$$

Here, ϕ_I is a parameter that depends on the repulsive potential constants, γ_A and γ_B are the surface free energy of material A and material B respectively, ϕ_V is a parameter that depends on the molar volume of the compounds. The full expression of this equation is given in Appendix A.

As stated by Wu [26], the utility of this equation is limited, because ϕ_I is an empirical parameter and its calculation remains questionable especially for polymers.

A similar expression of the work of adhesion was also proposed by Wu [26]:

$$W_{AB} = 2\varphi_{AB}(\gamma_A\gamma_B)^{1/2} \tag{4}$$

where φ_{AB} is a parameter that depends on the surface free energy and the molar volume of each compound. The full expression of Wu's equation is given in Appendix A.

However, this equation depends on the surface free energy which is obtained by time consuming experimental methods.

In this context, a relationship between solubility parameter and surface free energy was presented by Hildebrand in 1950 [15]:

$$\frac{\delta^2 v^{1/3}}{\gamma} = k. \tag{5}$$

In 1967, Gardon [27] asserted in his treatise that this equation reasonably holds for a variety of materials for which he assumed that $k = 16$. This constant k varies only between certain limits according to the type of molecules [16] and should be constant for a variety of materials [28].

We will use this relationship in Section 4 to develop equations of the work of adhesion as a function of the Hildebrand solubility parameter which we can estimate using molecular simulation.

2.2.3. The ideal tensile strength

The work of adhesion and the ideal tensile strength involve the same force by which two materials attract each other when an attempt is made to separate them. Whereas, the tensile strength divides this force by the cross section of the materials, the work of adhesion integrates this force through the distance between the materials. Gardon [27] defined the tensile strength σ_{AB}^{max} as the maximum stress that can support the interface between two materials A and B. He related it to the work of adhesion between two materials (A and B) separated by a potential equilibrium distance d_{AB}^0:

$$\sigma_{AB}^{max} = \frac{1.03W_{AB}}{d_{AB}^0}. \tag{6}$$

Gardon used Eq. (3) proposed by Girifalco and Good [25] into Eq. (5) and, by expressing the equilibrium distance d_{AB}^0 as the distance between the neighboring spherical sites of material A and material B, he ended up with the ideal tensile strength equation in terms of the solubility parameter:

$$\sigma_{AB}^{max} = 0.2452\phi_I{\phi_V}^{3/2}\delta_A\delta_B. \tag{7}$$

Here, σ_{AB}^{max} is in $J{\cdot}cm^{-3}$ and δ in $(J{\cdot}cm^{-3})^{1/2}$. These equations take into consideration the parameter ϕ_V which takes into account the different sizes of the interacting spherical sites.

Rowe [29] aimed at finding an expression for the ideal tensile strength in terms of the solubility parameter. He started with Gardon's expression (Eq. (6)) to obtain the ideal tensile strength using the work of adhesion. Then, he used Hildebrand's Eq. (5) with a k value $k = 16$ to substitute the surface free energy by the Hildebrand solubility parameter in Wu's Eq. (4). He ended up with the following expression:

$$\sigma_{AA}^{max} = 0.25\delta_A^2, \sigma_{BB}^{max} = 0.25\delta_B^2 \text{ and } \sigma_{AB}^{max} = 0.25\varphi_{AB}\delta_A\delta_B \quad \left(J\cdot cm^{-3}\right) \tag{8}$$

where σ_{AA}^{max} and σ_{BB}^{max} are the ideal tensile strength for compound A and compound B respectively, σ_{AB}^{max} is the maximum adhesive tensile strength between A and B.

The application of Rowe's model to real systems was partially conclusive at first because of the inaccuracy of the solubility parameter calculation approach that mixed Hoy and Van Krevelen group contribution methods [30]. Benali [31] adopted the same model but, instead of the group contribution methods, he used molecular simulation to calculate the solubility parameter. This approach provided better prediction of binary system affinity in accordance with experiments.

Furthermore, a closer examination of Rowe and Gardon's derivation shows two differences: the constant multiplier was approximated by Rowe from 0.2452 to 0.25. Furthermore, if we follow Rowe's derivation method from Gardon's [27] expression, we should obtain the following formula for the ideal tensile strength which differs from Rowe's Eq. (8) by the factor ϕ_V:

$$\sigma_{AB}^{max} = 0.2452\varphi_{AB}\delta_A\delta_B\phi_V^{1/2} \quad \left(J\cdot cm^{-3}\right). \tag{9}$$

The two equations (Eqs. (7) and (9)) are still based on the use of the constant $k = 16$ proposed by Gardon [27]. We will propose a more general expression in Subsection 4.1.

3. Materials and methods

3.1. Materials and their properties

The compounds chosen in this study are as follows: polyvinylpyrrolidone (PVP), microcrystalline cellulose (MCC) (Avicel PH102), hydroxypropyl-methylcellulose (HPMC), ethyl cellulose (EC), niflumic acid (NA), purified stearic acid (SA), polyethylene glycol (PEG), cellulose acetate (CA), nitrocellulose (NC) and water. The molar parachor of polymer was calculated using correlation (B.2) in Appendix B. For acids and water we used the structural contribution method of Sugden [32].

The properties of the different compounds are displayed in Table 1.

From Table 1, we can see that the agreement is reasonable between the values of the total surface free energy obtained by the parachor (see Appendix B) method and those estimated experimentally from the contact angle method.

The aqueous solution used in coating and agglomeration processes is a multicomposite polymer dispersion. This includes the film forming polymer, insoluble or unstable film additives or surfactants to promote spreading, and plasticizers to impart flexibility, improve flow and reduce brittleness. Thus, one of the major issues in the particle size enlargement process is the selection of suitable compounds and the elaboration of a stabilized dispersion (colloidal solution). The stability of these solutions strongly depends on the interactions between the constituents of the mixture in the presence of a solvent which is often water.

Once the coating or binder solution is sprayed onto the powders through the various unit processes, it will result in the formation of a continuous film on the surface of particles during the coating, or in the formation of solid bridges between the grains during agglomeration (see Fig. 1). The particles get closer during the drying process and the interparticle forces makes the particles eventually coalesce with each other, and cause the spheres to fuse, resulting in a coated film or solid bridges between the primary particles (see Fig. 2).

Table 1
Solubility parameter, surface free energy and density found in the literature.

Compounds	Density ($g \cdot cm^{-3}$)	Surface free energy ($mJ \cdot m^{-2}$). experiments		Surface free energy ($mJ \cdot m^{-2}$). parachor	Solubility parameter $(J \cdot cm^{-3})^{1/2}$	Molar volume v [a] ($cm^3 \cdot mol^{-1}$)
		γ	γ_d	γ	δ	
PVP	1.25[44]	53.6[47]	28.4[47]	47.65	–	90.56
MCC	1.59[12]	53.1[31]	42.4[31]	50.48	29.3[49]	204.02
HPMC	1.26[31]	34[30]	17[30]	36.05	22.8[47]	338.49
EC	1.27[45]	35.8[30]	25[30]	31.75	19–21[16]	387.87
NA	1.56[45]	45.9[30]	26.2[30]	52.83	23.8[50]	180.90
SA	0.847[12]	–	–	26.94	17.6[47]	335.87
PEG200	1.127[46]	46.7[48]	43.5[48]	44.95	24[16]	172.32
PEG400	1.127[46]	–	–	–	–	353.59
CA	1.31[12]	45.9[44]	–	42.64	24[16]	375.87
NC	1.6[44]	38[44]	–	48.13	21.7[16]	371.41
Water	0.997[12]	72[31]	21.8[31]	81.29	47.9[16]	18.05

PVP: polyvinylpyrrolidone, MCC: microcrystalline cellulose, HPMC: hydroxypropyl-methylcellulose, EC: ethyl cellulose, NA: niflumic acid, SA: stearic acid, PEG: polyethylene glycol, CA: cellulose acetate, NC: nitrocellulose.

[a] The molar volume of each monomer is calculated from the ratio of the molecular weight to the density.

The properties of the final product depend on the affinity between the surface of the powder and the pulverized solution. It depends also on the interactions between the different components (polymers, fatty acids, solvent…) involved in the formulation of the composite coating agent.

In this article, we used the experimental finding of Laboulfie [14] regarding the coating of solid particles by an aqueous solution containing HPMC as a matrix for film formation (67% of dried material), micronized SA as a hydrophobic filler (20% of dried material) and polyethylene glycol as a plasticizer (13% of dried material).

During polymeric solution preparation (see Fig. 3), the hot aqueous solution of HPMC is mixed with the PEG plasticizer and the SA hydrophobic filler. Then nucleation occurs as the particles gather together by affinity. Typically, hydrophobic SA particles gather away from water, whereas HPMC and PEG can dissolve in water. After cooling, the fine particles of SA will be stabilized by HPMC. HPMC polymer is able to form a gel network. This gel will entrap SA particles and prevent them from getting close in the range of attractive forces.

During film formation by drying, the evaporation of the interstitial water leads to the formation of liquid bridges between the HPMC polymer chains. The final composite film of HPMC and PEG incorporates crystal inclusions of PEG and SA [33] (see Fig. 3). The presence of crystals of SA in the interstitial space between the molecules of HPMC reduces the interactions between the polymer chains and, therefore, prevents their coalescence. An increase in the drying temperature leads to the formation of smaller crystals of PEG in the liquid bridges. Thus, the lack of contact between the polymer chains due to the presence of SA crystals is replaced by the contact between HPMC and PEG molecules. This will improve the plastic properties of the dry coating film.

3.2. Molecular simulation

For the computation of the solubility parameters, we run molecular simulations in the canonical ensemble NVT with the Forcite® module of the Material Studio Suite release 7 [34]. Simulations are run over 500 ps with a time step of 1 fs. The temperature is set at $T = 298$ K and controlled by using a Nose Hoover thermostat. The experimental densities listed in Table 1 are used to set the simulation box volume. Energy and pressure stability were checked. The last 50 ps is used for averaging potential energy components. The average cohesive energy is computed to derive the solubility parameter by using Eq. (2). The standard deviation method can be evaluated from the block averages' method [35].

Depending on the components, COMPASSII and PCFF forcefields were used with their predefined atom type parameters and the results were compared. Both molecular dynamic forcefields describe the energy of interaction by adding an intramolecular contribution accounting for bond stretching, bending and torsion, and an intermolecular contribution term accounting for Van der Walls and coulombian interactions. Van der Waals interaction was truncated by a spline function after 15.5 Å. For the coulombian interaction, partial charges were assigned by the predefined forcefield equilibration method, while the Ewald summation was used to account for the long range interactions.

4. Affinity prediction model for binary and ternary mixtures

The previous equations of the work of adhesion and the ideal tensile strength are only relevant to binary systems. In, this section, we will generalize these equations to our selected materials, and we will extend the ideal tensile strength to ternary systems. The resulting equations are then used to predict the affinity between granulation materials in binary and ternary systems.

4.1. Generalization of the work of adhesion and tensile strength formula

Rowe recognized that his model (Eq. (8)) was oversimplified and did not have a general validity [29]. We have already mentioned that Rowe's derivation should lead to Eq. (9) where a factor $\phi_V^{1/2}$ was omitted by Rowe. We can further generalize Rowe's equation by removing the

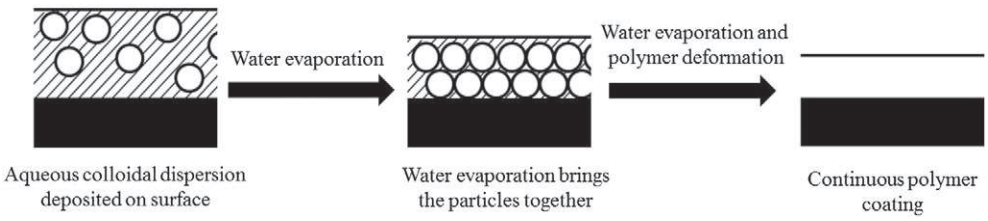

Fig. 2. Film formation during the evaporative phase. Figure adapted from [51].

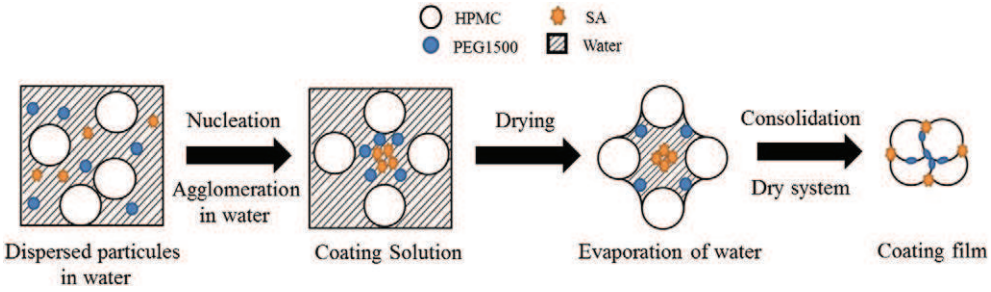

Fig. 3. Coating preparation steps of HPMC–SA–PEG1500 mixture placed in water, HPMC: hydroxypropyl-methylcellulose, SA: stearic acid, PEG1500: polyethylene glycol 1500.

assumption that $k = 16$: The appropriate choice of the factor k should depend on the compound of interest. Hence, if we consider the general form of Hildebrand relationship:

$$\delta = k'\left(\frac{\gamma}{v^{1/3}}\right)^{m} \text{ or } \delta^2 = k\left(\frac{\gamma}{v^{1/3}}\right)^{2m} \tag{10}$$

where $k' = k^{1/2}$ and m are constants that depend on the type of material, γ in dynes·cm^{-1}, δ in (cal·cm^{-3})$^{0.5}$, v in cm^3·mol^{-1}. We obtain the general expressions of the ideal tensile strength:

$$\sigma_{AA}^{\max} = 16.42\left(\frac{\delta_A}{k'_A}\right)^{1/m_A} \tag{11}$$

$$\sigma_{BB}^{\max} = 16.42\left(\frac{\delta_B}{k'_B}\right)^{1/m_B} \tag{12}$$

$$\sigma_{AB}^{\max} = 16.42\varphi_{AB}\phi_V^{1/2}\left(\frac{\delta_B}{k'_B}\right)^{1/2m_B}\left(\frac{\delta_A}{k'_A}\right)^{1/2m_A} \tag{13}$$

$$\varphi_{AB} = 2\left(\frac{x_A^d x_B^d}{g_A x_A^d + g_B x_B^d} + \frac{x_A^p x_B^p}{g_A x_A^p + g_B x_B^p}\right). \tag{14}$$

$$\text{With } x_i^d = \left(\frac{\delta_d}{\delta}\right)^{1/m}, \quad x_i^p = 1 - x_i^d \tag{15}$$

$$g_A = \frac{\delta_A^{1/m_A} k'^{1/m_B}_B v_A^{1/3}}{\delta_B^{1/m_B} k'^{1/m_A}_A v_B^{1/3}} \text{ and } g_B = \frac{1}{g_A} \tag{16}$$

where $\sigma_{AB}^{\max}$ is in J·cm^{-3} and δ in cal$^{1/2}$·cm$^{-3/2}$, x_i^p and x_i^d are the polar and the nonpolar fraction of material i (i = A *or* B). We use Eq. (13) to calculate the adhesive tensile strength for binary mixtures. For the same material, we use Eq. (11) describing mutual cohesion. Here k' and m have to be determined for each type of material.

Following the same route of computation, the work of adhesion described by Eq. (4) becomes:

$$W_{AB} = 2\varphi_{AB}\left(\frac{\delta_A}{k'_A}\right)^{1/2m_A}\left(\frac{\delta_B}{k'_B}\right)^{1/2m_B}(v_A v_B)^{1/6} \tag{17}$$

where W_{AB} is in mJ·m^{-2}, δ in cal$^{1/2}$·cm$^{-3/2}$ and v in cm^{-3}·mol^{-1}.

4.2. Extension of the ideal tensile strength model to ternary systems

In this section, we extend relationship (9) proposed by Gardon for the ideal tensile strength for a binary mixture in vacuum to ternary mixtures where the substrates are dispersed in a third medium.

According to Israelachvili [36], the work of adhesion between two products A and B in a medium C is related to the process of building A–B agglomerates (adhesion of A and B alone) in a medium C (cohesion of C alone) against the solubilization of A and B in C (work of adhesion of A and C, and B and C respectively). It has the following form:

$$W_{ACB} = W_{AB} + W_{CC} - W_{AC} - W_{BC}. \tag{18}$$

Similarly, the work of cohesion of A in a medium C is given by:

$$W_{ACA} = W_{AA} + W_{CC} - 2W_{AC}. \tag{19}$$

By implementing the equation of work of adhesion in a third medium given by Israelachvili [36] in the process of resolution followed by Gardon [27], we derive the relationship between the total work of adhesion W_{ACB} and the ideal tensile strength $\sigma_{ACB}^{\max}$ in third medium, along with an expression of the equilibrium distance at zero potential energy d_{ACB}^0:

$$\sigma_{ACB}^{\max} = \frac{1.0263 W_{ACB}}{d_{ACB}^0} \left(\text{J}\cdot\text{cm}^{-3}\right) \tag{20}$$

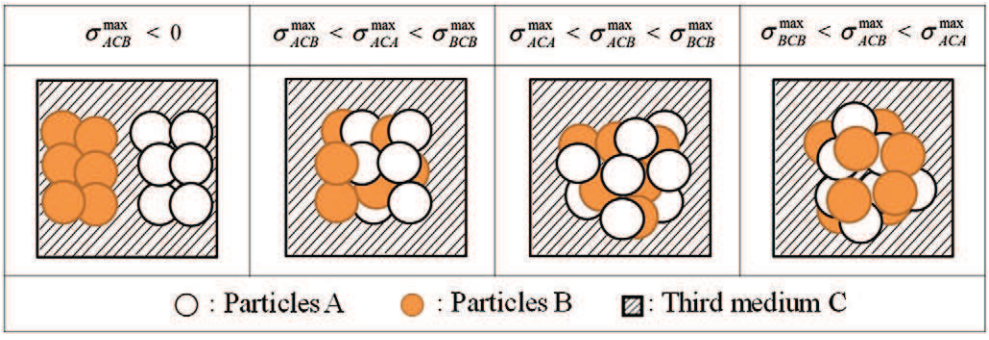

Fig. 4. Interactions predicted between particles A and particles B in a third medium C based on the tensile strength approach.

Table 2
Solubility parameters calculated by different methods.

Solubility parameter $(J\cdot cm^{-3})^{1/2}$	Group contribution		Molecular simulation forcefields				Exp.
	HSPiP		COMPASSII		PCFF		
Compounds	δ	δ_d	δ	δ_d	δ	δ_d	δ
PVP	21.2	18.5	21.12 ± 0.16	19.45 ± 0.18	19.77 ± 0.11	17.60 ± 0.10	–
MCC	29.2	18.8	29.98 ± 0.24	17.04 ± 0.32	28.12 ± 0.13	20.71 ± 0.16	29.3[49]
HPMC	20.2	17.1	20.68 ± 0.13	17.03 ± 0.14	20.98 ± 0.10	18.39 ± 0.09	22.8[47]
EC	18.8	16.7	19.61 ± 0.15	18.73 ± 0.15	16.08 ± 0.08	15.46 ± 0.07	19–21[16]
NA	21.9	19.3	25.40 ± 0.19	21.97 ± 0.23	23.73 ± 0.56	20.23 ± 0.43	23.8[50]
SA	17.5	16.3	18.61 ± 0.22	16.75 ± 0.26	19.89 ± 0.26	17.72 ± 0.28	17.6[47]
PEG200	24.4	16.4	26.54 ± 0.22	19.27 ± 0.24	26.18 ± 0.39	20.91 ± 0.32	24[16]
PEG400	19.0	14.6	22.88 ± 0.24	20.17 ± 0.24	24.07 ± 0.16	22.51 ± 0.17	–
CA	24.4	18.0	20.98 ± 0.22	17.74 ± 0.21	23.17 ± 0.19	21.54 ± 0.18	24[16]
NC	25.0	17.9	22.34 ± 0.41	17.00 ± 0.28	110.13 ± 0.13	26.88 ± 0.17	21.7[16]
Water	47.8	15.5	47.78 ± 0.59	–	47.33 ± 0.20	5.89 ± 1.98	47.9[16]

PVP: polyvinylpyrrolidone, MCC: microcrystalline cellulose, HPMC: hydroxypropyl-methylcellulose, EC: ethyl cellulose, NA: niflumic acid, SA: stearic acid, PEG: polyethylene glycol, CA: cellulose acetate, NC: nitrocellulose.

$$d^0_{ACB} = 0.629 * 10^{-8}\left(\frac{\sigma^{max}_{AB}\left(v_A^{1/3}+v_B^{1/3}\right)^9+\sigma^{max}_{CC}\left(2v_C^{1/3}\right)^9-\sigma^{max}_{AC}\left(v_A^{1/3}+v_C^{1/3}\right)^9-\sigma^{max}_{BC}\left(v_A^{1/3}+v_C^{1/3}\right)^9}{\sigma^{max}_{AB}\left(v_A^{1/3}+v_B^{1/3}\right)^3+\sigma^{max}_{CC}\left(2v_C^{1/3}\right)^3-\sigma^{max}_{AC}\left(v_A^{1/3}+v_C^{1/3}\right)^3-\sigma^{max}_{BC}\left(v_B^{1/3}+v_C^{1/3}\right)^3}\right)^{(1/6)}. \quad (21)$$

The detailed demonstration is given in Appendix B.
Using Eq. (18), Eq. (20) can be rewritten as:

$$\sigma^{max}_{ACB} = \frac{1.0263(W_{AB}+W_{CC}-W_{AC}-W_{BC})}{d^0_{ACB}} = \frac{\left(d^0_{AB}\sigma^{max}_{AB}+d^0_{CC}\sigma^{max}_{CC}-d^0_{AC}\sigma^{max}_{AC}-d^0_{BC}\sigma^{max}_{BC}\right)}{d^0_{ACB}}. \quad (22)$$

Combining Eqs. (21) and (22), we obtain:

$$\sigma^{max}_{ACB} = \frac{\left(\sigma^{max}_{AB}\left(v_A^{1/3}+v_B^{1/3}\right)+2\sigma^{max}_{CC}\left(v_C^{1/3}\right)-\sigma^{max}_{AC}\left(v_A^{1/3}+v_C^{1/3}\right)-\sigma^{max}_{BC}\left(v_B^{1/3}+v_C^{1/3}\right)\right)}{\left(\frac{\sigma^{max}_{AB}\left(v_A^{1/3}+v_B^{1/3}\right)^9+\sigma^{max}_{CC}\left(2v_C^{1/3}\right)^9-\sigma^{max}_{AC}\left(v_A^{1/3}+v_C^{1/3}\right)^9-\sigma^{max}_{BC}\left(v_A^{1/3}+v_C^{1/3}\right)^9}{\sigma^{max}_{AB}\left(v_A^{1/3}+v_B^{1/3}\right)^3+\sigma^{max}_{CC}\left(2v_C^{1/3}\right)^3-\sigma^{max}_{AC}\left(v_A^{1/3}+v_C^{1/3}\right)^3-\sigma^{max}_{BC}\left(v_B^{1/3}+v_C^{1/3}\right)^3}\right)^{(1/6)}}. \quad (23)$$

According to Eq. (20), the ideal tensile strength σ^{max}_{ACB} is proportional to the work of adhesion W_{ACB}, thus, by analogy with the conclusions of Barra [30] and Benali [31], we can state that in a ternary system (see also Fig. 4):

- If $\sigma^{max}_{ACB} > 0$: one of the compounds is partially spread over the other, and C (water for example) does not spread between A and B;
- If $\sigma^{max}_{ACB} < 0$: medium C will displace compound B and "spread on" or "totally wet" the surface of A
- If $\sigma^{max}_{ACB} < \sigma^{max}_{ACA} < \sigma^{max}_{BCB}$: both compounds tend to mix, no interaction between them
- If $\sigma^{max}_{ACA} < \sigma^{max}_{ACB} < \sigma^{max}_{BCB}$: compound A will surround compound B in solvent C
- If $\sigma^{max}_{BCB} < \sigma^{max}_{ACB} < \sigma^{max}_{ACA}$: compound B will surround compound A in solvent C.

The same predictions were stated by Israelachvili [36] but in terms of the work of adhesion of two compounds placed in a third medium.

5. Model application and discussion

Before applying the above equations to predict the affinity in binary and ternary systems, we discuss the values of the solubility parameters.

5.1. Solubility parameter calculated by different methods

Table 2 compares experimental solubility parameters with those predicted by the Yamamoto method [23] and by molecular simulation.

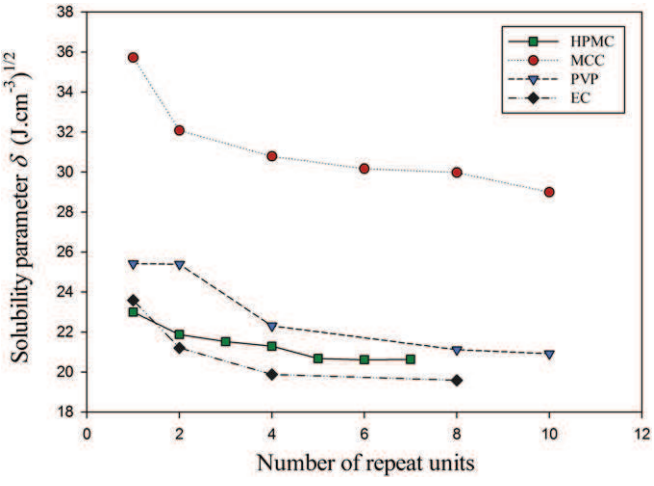

Fig. 5. Variation of Hildebrand solubility parameter versus number of repetition unit of polymers.

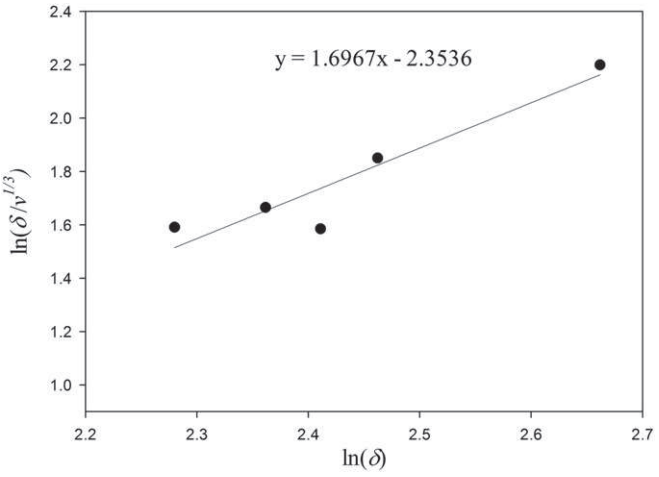

Fig. 6. Logarithm of the ratio $\gamma/v^{1/3}$ plotted against the logarithm of the Hildebrand solubility parameters δ. δ in $(cal\cdot cm^{-3})^{1/2}$ and surface tension γ in $mJ\cdot m^{-2}$. γ and δ of celluloses derivatives are obtained from literature.

Table 2 compares experimental solubility parameters with those predicted by the Yamamoto method [23] and by molecular simulation.

Table 3
Work of cohesion in $mJ \cdot m^{-2}$ calculated using different correlations.

	Solubility parameter $(J \cdot cm^{-3})^{1/2}$		Work of cohesion W_{AA} $(mJ \cdot m^{-2})$					
	COMPASSII		Gardon[27,28] $_{k'} = 4\ m = 0.5\ k' = 4.38$[a]	Hildebrand[15] $k' = 4.1\ m = 0.43$	Sheldon[39] Eq (24) $k' = 5.93\ m = 0.45$	Bonn[38] $k' = 3.39\ m = 0.5$	This work Eq (25) $k' = 4\ m = 0.59$	$W_{AA} = 2\gamma$ Exp.[b]
	δ	δ_d						
PVP	21.12	19.45	59.75	76.82	30.75	83.19	44.86	107.2
MCC	29.98	17.04	158.01	227.69	87.90	219.99	106.73	106.2
HPMC	20.68	17.03	89.01	113.65	45.59	123.92	67.26	68.0
EC	19.61	18.73	83.75	105.10	42.40	116.60	64.31	71.6
NA	25.40	21.97	108.96	148.76	58.42	151.70	77.38	91.8
SA	18.61	16.75	71.89	88.70	35.97	100.09	56.09	–
PEG200	26.54	19.27	117.05	162.10	63.38	162.97	82.03	93.4
PEG400	22.88	20.17	110.55	145.87	57.91	153.91	81.02	–
Water	47.33[c]	5.89[c]	175.48	293.39	108.05	244.32	103.25	144.0

PVP: polyvinylpyrrolidone, MCC: microcrystalline cellulose, HPMC: hydroxypropyl-methylcellulose, EC: ethyl cellulose, NA: niflumic acid, SA: stearic acid, PEG: polyethylene glycol.
[a] Only for water.
[b] Calculated using the experimental interfacial tension γ given in Table 1.
[c] PCFF forcefield.

For the molecular simulation of polymers, the number of repeating unit was chosen so that the solubility parameter remains constant in case of further increasing of the repeating unit. Results are displayed in Fig. 5. The number of repetition unit was fixed to 8 for MCC, PVP and EC, and 5 for HPMC.

The average value of the cohesive energy density is obtained for all compounds from the last 50 picoseconds (ps) of the 500 ps dynamic simulation, spanning 500,000 time steps. However, getting a good estimation of the average standard deviation in molecular dynamics simulation requires typically over several millions of time steps, which are practically difficult to obtain in a reasonable lapse of time. Indeed, the average standard deviation must be computed over uncorrelated frames. This can be achieved by using the block average variance method [35]. Its application to simple system, like Lennard Jones fluids [37] shows that the average standard deviation over uncorrelated frames is at least one order of magnitude greater than the standard deviation computed directly from the molecular dynamics frame trajectory. Its application to the real systems we studied was not possible in a reasonable lapse of time; therefore we estimated the average standard deviation as ten times the standard error given by Forcite [34].

The number of molecules distributed initially in the simulation cell has very little effect on the values of the solubility parameters [31]. Generally four polymer chains are sufficient, although for very high molecular weights even one chain can be adequate [24]. We have 10 molecules per cell for PVP, MCC, PEG400 and SA, 8 molecules per cell for HPMC, 6 molecules per cell for CA and NC, 30 molecules per cell for NA, 40 molecules per cell for PEG200 and 100 molecules per cell for water. Larger number will increase the computational effort.

Table 2 shows that experimental Hildebrand solubility parameters are close to the COMPASSII forcefield and HSPiP results. Concerning water, only the PCFF forcefield gives a dispersive contribution to the solubility parameter, consequently, in this study, we will compare the solubility parameter predictions obtained from HSPiP and COMPASSII forcefield, except for water where we will use PCFF forcefield values.

Table 4
Cohesion work (diagonal) and adhesion work in $mJ \cdot m^{-2}$ in the binary mixture calculated using the solubility parameter obtained from COMPASSII forcefield.

Compounds	PVP	MCC	HPMC	EC	NA	SA	PEG200	PEG400
PVP	83.19							
MCC	72.85	106.73						
HPMC	66.87	69.40	67.26					
EC	64.95	56.39	61.05	64.31				
NA	90.58	91.02	68.21	63.14	108.96			
SA	76.32	70.78	66.11	63.00	81.00	71.89		
PEG200	73.29	87.10	71.39	60.92	81.62	71.71	82.03	
PEG400	79.51	74.53	71.79	68.46	82.52	75.96	76.60	81.02

PVP: polyvinylpyrrolidone, MCC: microcrystalline cellulose, HPMC: hydroxypropyl-methylcellulose, EC: ethyl cellulose, NA: niflumic acid, SA: stearic acid, PEG: polyethylene glycol.

Table 5
Cohesion work (diagonal) and adhesion work in $mJ \cdot m^{-2}$ in the binary mixture calculated using the solubility parameter obtained from HSPiP method.

Compounds	PVP	MCC	HPMC	EC	NA	SA	PEG200	PEG400
PVP	83.82							
MCC	84.33	102.06						
HPMC	65.97	68.66	64.63					
EC	61.03	61.97	61.65	59.87				
NA	82.32	82.02	65.77	61.10	81.00			
SA	69.15	65.91	61.50	59.14	68.82	63.57		
PEG200	67.36	79.83	63.25	57.87	66.27	56.63	71.12	
PEG400	59.60	65.96	60.61	57.08	59.31	54.63	62.68	59.10

PVP: polyvinylpyrrolidone, MCC: microcrystalline cellulose, HPMC: hydroxypropyl-methylcellulose, EC: ethyl cellulose, NA: niflumic acid, SA: stearic acid, PEG: polyethylene glycol.

Table 6
The ideal tensile strength in binary mixtures in $J \cdot cm^{-3}$ calculated using the solubility parameter obtained from COMPASSII forcefield.

Compounds	PVP	MCC	HPMC	EC	NA	SA	PEG200	PEG400
PVP	152.07							
MCC	115.18	148.66						
HPMC	95.73	88.53	79.14					
EC	90.44	70.17	70.20	72.31				
NA	146.48	129.32	88.60	79.97	157.98			
SA	109.45	90.42	77.88	72.54	105.37	84.81		
PEG200	119.59	124.73	93.41	77.71	119.30	93.97	120.87	
PEG400	112.84	94.33	83.85	78.16	106.34	88.84	99.42	93.96

PVP: polyvinylpyrrolidone, MCC: microcrystalline cellulose, HPMC: hydroxypropyl-methylcellulose, EC: ethyl cellulose, NA: niflumic acid, SA: stearic acid, PEG: polyethylene glycol.

Table 7
The ideal tensile strength in binary mixtures in $J \cdot cm^{-3}$ calculated using the solubility parameter obtained from HSPiP method.

Compounds	PVP	MCC	HPMC	EC	NA	SA	PEG200	PEG400
PVP	153.23							
MCC	133.34	142.16						
HPMC	94.45	87.58	76.04					
EC	84.98	77.11	70.89	67.31				
NA	133.13	116.54	85.44	77.38	117.45			
SA	99.15	84.20	72.46	68.09	89.52	74.99		
PEG200	109.92	114.33	82.77	73.82	96.87	74.21	104.80	
PEG400	84.58	83.48	70.79	65.17	76.43	63.90	81.35	68.53

PVP: polyvinylpyrrolidone, MCC: microcrystalline cellulose, HPMC: hydroxypropyl-methylcellulose, EC: ethyl cellulose, NA: niflumic acid, SA: stearic acid, PEG: polyethylene glycol.

5.2. Relationship between solubility parameter and surface free energy for cellulose derivatives

For computing the work of adhesion (Eq. (17)), we need to select constants k' and m that come from Eq. (10). Hildebrand [15] used $k' = 4.1$ and $m = 0.43$ when δ is in $cal^{1/2} \cdot cm^{-3/2}$. Gardon [27] proposed $k = 16$ ($k' = 4$) and $m = 0.5$ for organic acids and molten metals, which gave an error on the ideal tensile strength usually below 25% for the systems he studied. For water he proposed ($k' = 4.376$) and $m = 0.5$. From simple statistical thermodynamic considerations, Bonn [38] related the solubility of polymers to the surface tension and obtained $k = 11.5$ ($k' = 3.39$) by regression analysis. For compounds which do not contain OH, COOH and a COH groups, Sheldon [39] proposed $k = 14.0$ ($k' = 3.74$) with $m = 1$, and $k = 35.13$ ($k' = 5.927$) with $m = 0.45$ otherwise:

$$\delta^2 = \begin{cases} 14\gamma/v^{1/3} & if \;\; nOH + nCOOH + nCOH = 0 \\ 35.13\gamma/v^{0.45} & otherwise \end{cases}. \tag{24}$$

For cellulose polymers, we regress an expression by using the Hildebrand solubility parameter values over the data of 5 compounds; MCC, HPMC, EC, CA and NC. The theoretical best fit line is shown in Fig. 6.

The following expression was obtained:

$$\delta = 4.00 \left(\gamma/v^{1/3}\right)^{0.59} \left(cal \cdot cm^{-3}\right)^{1/2}. \tag{25}$$

Table 3 collects the prediction of the work of cohesion calculated using the various correlations cited above and compares them with the experimental values of the work of cohesion $W_{AA} = 2\gamma$ (for when A = B). The solubility parameter in the correlations is obtained by molecular simulation using the COMPASSII forcefield.

In Table 3, the results obtained using Eq. (25) are close to the experimental values for MCC, HPMC, EC and PEG. Gardon's [28] correlation is close to the experimental values for acids and water. For PVP, Bonn's [38] correlation is the closest. Therefore, we select the corresponding best fit values: $k' = 4$ for acids, $k' = 3.01$ for PVP, $k' = 4.376$ for water, and Eq. (25) for the celluloses derivatives and PEG.

Table 8
Interactions predicted for PVP and MCC.

A	B											
	PVP						MCC					
	Exp. obs.	W_{AB} exp.	W_{AB} HSPiP	σ_{AB} HSPiP	W_{AB} compassII	σ_{AB} compassII	Exp. obs.	W_{AB} exp.	W_{AB} HSPiP	σ_{AB} HSPiP	W_{AB} compassII	σ_{AB} compassII
PVP	–	–	–	–	–	–		M	O	M	M	M
MCC		M	X	M	M	M	–	–	–	–	–	–
HPMC		O	O	O	M	O	O[31]	O	O	O	O	O
EC		O	O	O	O	O		O	O	O	M	M
NA		O	O	O	X	M		M	O	M	M	M
SA			O	O	O	O			O	O	M	O
PEG200		M	M	O	M	M		O	O	O	O	O
PEG400			O	O	M	O			O	O	M	O

PVP: polyvinylpyrrolidone, MCC: microcrystalline cellulose, HPMC: hydroxypropyl-methylcellulose, EC: ethyl cellulose, NA: niflumic acid, SA: stearic acid, PEG: polyethylene glycol.
O: A surrounds B, X: B surrounds A, M: no interactions between A and B.

Table 9
Interactions predicted for HPMC and EC.

A	B											
	HPMC						EC					
	Exp. obs.	W_{AB} exp.	W_{AB} HSPiP	σ_{AB} HSPiP	W_{AB} compassII	σ_{AB} compassII	Exp. obs.	W_{AB} exp.	W_{AB} HSPiP	σ_{AB} HSPiP	W_{AB} compassII	σ_{AB} compassII
PVP		X	X	X	M	X		X	X	X	X	X
MCC	X[31]	X	X	X	X	X		X	X	X	M	M
HPMC	–	–	–	–	–	–	M[30]	M	X	X	M	M
EC	M[30]	M	O	O	M	M	–	–	–	–	–	–
NA	X[30]	X	X	X	X	X	M[30]	X	X	X	M	X
SA			M	M	M	M			M	X	M	X
PEG200	X[14]	M	M	X	X	X		M	M	X	M	X
PEG400			O	O	X	X			M	M	X	X

PVP: polyvinylpyrrolidone, MCC: microcrystalline cellulose, HPMC: hydroxypropyl-methylcellulose, EC: ethyl cellulose, NA: niflumic acid, SA: stearic acid, PEG: polyethylene glycol.
O: A surrounds B, X: B surrounds A, M: no interactions between A and B.

Table 10
Interactions predicted for NA and SA.

A	B											
	NA						SA					
	Exp. obs.	W_{AB} exp.	W_{AB} HSPiP	σ_{AB} HSPiP	W_{AB} compassII	σ_{AB} compassII	Exp. obs.	W_{AB} exp.	W_{AB} HSPiP	σ_{AB} HSPiP	W_{AB} compassII	σ_{AB} compassII
PVP		X	X	X	O	M			X	X	X	X
MCC		M	X	M	M	M			X	X	M	X
HPMC	O[30]	O	O	O	O	O			M	M	M	M
EC	M[30]	O	O	O	M	O			M	O	M	O
NA	–	–	–	–	–	–			X	X	X	X
SA			O	O	O	O	–	–	–	–	–	–
PEG200		M	M	M	M	M	M[14]		M	M	M	X
PEG400			O	O	O	O			M	M	X	X

PVP: polyvinylpyrrolidone, MCC: microcrystalline cellulose, HPMC: hydroxypropyl-methylcellulose, EC: ethyl cellulose, NA: niflumic acid, SA: stearic acid, PEG: polyethylene glycol.
O: A surrounds B, X: B surrounds A, M: no interactions between A and B.

5.3. Prediction of the interactions in binary mixture

By using the k' and m values in Eq. (17), we calculate the work of adhesion and cohesion in a binary system. The results obtained by molecular simulations and by Yamamoto's molecular breaking method (HSPiP) are presented in Tables 4 and 5 respectively.

We can also calculate the ideal tensile strength in binary mixtures by using Eq. (13). The ideal tensile strength values obtained by molecular simulation are shown in Table 6, and those obtained using the Yamamoto's molecular breaking method (HSPiP) are presented in Table 7.

By comparing the adhesion and cohesion work values (Tables 4 and 5) and the ideal tensile strength results (Tables 6 and 7), we predict the affinity between the different compounds (Tables 8, 9, 10 and 11). The adhesive and the tensile approach being derived from the same core show similar predictions.

In all cases, we have $W_{HPMC-HPMC} < W_{HPMC-NA} < W_{NA-NA}$, this means that HPMC will adhere over the particles of NA. Moreover, as first observed experimentally by Barra [30], and recently reviewed by Benali [31], HPMC particles surround NA particles.

According to the work of adhesion predictions obtained on the basis of molecular simulation, the particles of EC interact neither with NA nor with HPMC (Table 9). This was also observed by Barra [30]. However, the tensile approach predicts that the particles of EC tend to adhere over the particles of NA (Table 9). This suggests that the adhesion approach gives more accurate predictions than the tensile approach. It's worth mentioning here that Barra observed also a low interaction between NA and EC for medium sized particles, where EC tends to adhere over the particle of NA, which may explain the disagreement between the predictions obtained with the adhesion approach and those obtained with the tensile strength approach in the case of the couple EC–NA.

Table 11
Interactions predicted for PEG200 and PEG400.

A	B											
	PEG200						PEG400					
	Exp. obs.	W_{AB} exp.	W_{AB} HSPiP	σ_{AB} HSPiP	W_{AB} compassII	σ_{AB} compassII	Exp. obs.	W_{AB} exp.	W_{AB} HSPiP	σ_{AB} HSPiP	W_{AB} compassII	σ_{AB} compassII
PVP		M	M	X	M	M			X	X	M	X
MCC		X	X	X	X	X			X	X	M	X
HPMC	O[14]	M	M	O	O	O			X	X	O	O
EC		M	M	O	M	O			M	M	O	O
NA		M	M	M	M	M			X	X	X	X
SA	M[14]		M	M	M	O			M	M	O	O
PEG200	–	–	–	–	–	–			X	X	M	X
PEG400			O	O	M	O	–	–	–	–	–	–

PVP: polyvinylpyrrolidone, MCC: microcrystalline cellulose, HPMC: hydroxypropyl-methylcellulose, EC: ethyl cellulose, NA: niflumic acid, SA: stearic acid, PEG: polyethylene glycol.
O: A surrounds B, X: B surrounds A, M: no interactions between A and B.

Table 12
Cohesion work (diagonal) and adhesion work in $mJ \cdot m^{-2}$ of the compounds dispersed in water, calculated using the solubility parameter obtained from COMPASSII and PCFF forcefields.

Compounds	PVP	MCC	HPMC	EC	NA	SA	PEG200	PEG400
PVP	181.54							
MCC	114.68	92.04						
HPMC	162.00	108.01	159.17					
EC	174.51	109.43	167.39	185.08				
NA	166.24	110.16	140.65	150.01	161.93			
SA	174.22	112.16	160.79	172.11	156.21	169.34		
PEG200	150.65	107.94	145.53	149.49	136.29	148.62	138.40	
PEG400	176.76	115.26	165.82	176.92	157.08	172.76	152.86	177.17

PVP: polyvinylpyrrolidone, MCC: microcrystalline cellulose, HPMC: hydroxypropyl-methylcellulose, EC: ethyl cellulose, NA: niflumic acid, SA: stearic acid, PEG: polyethylene glycol.

Table 13
Cohesion work (diagonal) and adhesion work in $mJ \cdot m^{-2}$ of the compounds dispersed in water, calculated using the solubility parameter obtained from HSPiP.

Compounds	PVP	MCC	HPMC	EC	NA	SA	PEG200	PEG400
PVP	119.55							
MCC	88.89	75.45						
HPMC	114.55	86.07	126.06					
EC	115.06	84.83	128.53	132.20				
NA	120.80	89.33	117.10	117.88	122.23			
SA	122.11	87.70	127.31	130.40	124.53	133.76		
PEG200	100.45	81.75	109.19	109.26	102.11	106.95	101.57	
PEG400	107.68	82.87	121.54	123.46	110.14	119.94	108.12	119.53

PVP: polyvinylpyrrolidone, MCC: microcrystalline cellulose, HPMC: hydroxypropyl-methylcellulose, EC: ethyl cellulose, NA: niflumic acid, SA: stearic acid, PEG: polyethylene glycol.

Moreover, the predictive results based upon both approaches (tensile strength and work of adhesion approach) indicate that HPMC would be a good binder for MCC substrate (Table 9) and consequently will produce rigid agglomerates. In their work on the interactions between HPMC and MCC, Benali [31] and Lovorka et al. [40] arrived to the same conclusion.

However, no interactions are observed in the case of HPMC–SA mixture which may results in friable agglomerate or coating film. To improve the properties of this mixture, one way is to add another compound compatible with SA and HPMC. Predictions obtained using molecular simulation show good affinity between PEG400 and both HPMC and SA (see Table 11). One could suspect that the addition of PEG400 to the SA–HPMC mixture should indirectly improve the consistency of the resulting agglomerate. This actually corresponds to the conclusions of Laboulfie et al. [33] where they stated that adding PEG to the HPMC–SA mixture will enhance the mechanical properties of the resulting composite coating.

In the light of the previous analyses, we conclude that the predictions obtained on the basis of molecular simulation calculations reproduce the available experimental observations, especially in the case of the adhesion work approach.

5.4. Prediction of the interactions in aqueous system: dispersion of substrate in a third medium

The work of adhesion and cohesion of different polymers and acids placed in water are calculated using the Israelachivili's relationships (18) and (19). The results based upon molecular simulation are presented in Table 12, and those obtained using the Yamamoto's molecular breaking method (HSPiP) are presented in Table 13.

We notice that the work of adhesion is positive for all the materials. Following Israelachivili's [36] conclusions, all the compounds should aggregate in water; furthermore, the water doesn't penetrate between the compounds which means that there is a spreading of one of the compounds over the other, or that the two compounds will self-associate in water without interacting. This can be explained by the high cohesive energy between water molecules, i.e. the interactions between them are much more attractive than their attraction with the other molecules.

The ideal tensile strength in ternary mixtures is calculated by using Eq. (23). The results based upon molecular simulation are presented in Table 14 and those obtained using the Yamamoto's molecular breaking method (HSPiP) are presented in Table 15.

First, we notice that the cohesion work and adhesion work in water obtained using the HSPiP data are much smaller than those obtained with COMPASSII and PCFF forcefield data. We state that this happens because the PCFF forcefield underestimates the dispersive contribution of the solubility parameter of water compared to HSPiP (see Table 2).

Regarding the prediction of affinity, for all methods, MCC has the lowest work of adhesion and cohesion in water, this imply that for all the mixtures, MCC will most likely adhere on the surface of the other compounds when they are dispersed in water.

The magnitude of interaction and therefore the affinity between compound A and compound B in a medium C is proportional to minus W_{BAC} ($W_{BAC} = W_{ACA} - W_{ACB}$). This also means that, in the presence of water, if minus W_{BAC} is high, the film formed in the surface of the stronger cohesive material will be thicker; this is identified in the case of the couple MCC–EC where minus $W_{MCC-EC-Water}$ is the highest (Table 12).

Table 14
The ideal tensile strength in ternary mixtures in $J \cdot cm^{-3}$ of the compounds dispersed in water, calculated using the solubility parameter obtained from COMPASSII and PCFF forcefields.

Compounds	PVP	MCC	HPMC	EC	NA	SA	PEG200	PEG400
PVP	347.85							
MCC	174.82	115.83						
HPMC	237.51	129.15	186.14					
EC	251.79	129.36	194.13	212.39				
NA	272.13	146.06	179.71	190.08	230.28			
SA	255.73	135.19	188.86	200.41	201.09	199.8		
PEG200	250.37	144.06	188.00	191.34	194.47	192.97	199.70	
PEG400	256.15	138.00	192.88	203.80	200.10	201.82	196.44	204.99

PVP: polyvinylpyrrolidone, MCC: microcrystalline cellulose, HPMC: hydroxypropyl-methylcellulose, EC: ethyl cellulose, NA: niflumic acid, SA: stearic acid, PEG: polyethylene glycol.

Table 15
The ideal tensile strength in ternary mixtures in $J \cdot cm^{-3}$ of the compounds dispersed in water, calculated using the solubility parameter obtained from HSPiP method.

Compounds	PVP	MCC	HPMC	EC	NA	SA	PEG200	PEG400
PVP	216.01							
MCC	128.03	91.87						
HPMC	158.70	97.75	140.85					
EC	155.78	93.73	140.93	142.42				
NA	189.93	114.04	144.22	142.08	169.4			
SA	171.04	100.22	143.06	143.87	155.25	151.84		
PEG200	156.50	103.41	134.05	131.13	139.39	131.57	139.40	
PEG400	146.84	92.52	133.99	133.52	133.24	132.52	131.31	130.34

PVP: polyvinylpyrrolidone, MCC: microcrystalline cellulose, HPMC: hydroxypropyl-methylcellulose, EC: ethyl cellulose, NA: niflumic acid, SA: stearic acid, PEG: polyethylene glycol.

Table 16
Interactions predicted for PVP and MCC.

A	B							
	PVP				MCC			
	W_{ACB} CompassII	σ_{ACB} CompassII	W_{ACB} HSPiP	σ_{ACB} HSPiP	W_{ACB} CompassII	σ_{ACB} CompassII	W_{ACB} HSPiP	σ_{ACB} HSPiP
PVP	–	–	–	–	X	X	X	X
MCC	O	O	O	O	–	–	–	–
HPMC	O	O	M	O	X	X	X	X
EC	M	O	M	O	X	X	X	X
NA	O	O	X	O	X	X	X	X
SA	O	O	X	O	X	X	X	X
PEG200	O	O	M	O	X	X	X	X
PEG400	M	X	M	O	X	X	X	X

PVP: polyvinylpyrrolidone, MCC: microcrystalline cellulose, HPMC: hydroxypropyl-methylcellulose, EC: ethyl cellulose, NA: niflumic acid, SA: stearic acid, PEG: polyethylene glycol.
O: A surrounds B, X: B surrounds A, M: no interactions between A and B.

On the basis of the previous tables (Tables 12, 13, 14 and 15), we can predict the affinity of our ternary systems (Tables 16, 17, 18 and 19).

Although they differ from the type of input data that they use (HSPiP vs. COMPASSII/PCFF forcefield), both solubility parameter calculation methods tend to give similar predictions.

Overall, the affinities, obtained through the ideal tensile strength and the work of adhesion based upon molecular simulation, are similar in 75% of the systems.

As expected, because of their low cohesion strength in water, MCC molecules surround the other compounds (Table 16). This also can be explained by the high hydrophilic character of the MCC.

Table 17
Interactions predicted for HPMC and EC.

A	B							
	HPMC				EC			
	W_{ACB} CompassII	σ_{ACB} CompassII	W_{ACB} HSPiP	σ_{ACB} HSPiP	W_{ACB} CompassII	σ_{ACB} CompassII	W_{ACB} HSPiP	σ_{ACB} HSPiP
PVP	X	X	M	X	M	X	M	X
MCC	O	O	O	O	O	O	O	O
HPMC	–	–	–	–	O	O	O	O
EC	X	X	X	X	–	–	–	–
NA	M	M	M	X	M	M	M	M
SA	X	X	X	X	O	O	M	X
PEG200	O	X	O	M	O	M	O	M
PEG400	X	X	O	O	M	M	O	O

PVP: polyvinylpyrrolidone, MCC: microcrystalline cellulose, HPMC: hydroxypropyl-methylcellulose, EC: ethyl cellulose, NA: niflumic acid, SA: stearic acid, PEG: polyethylene glycol.
O: A surrounds B, X: B surrounds A, M: no interactions between A and B.

Also, in the case of HPMC–SA, whereas no interactions are observed between SA and HPMC in the absence of water (Table 9), HPMC will adhere on the surface of SA (Table 17) when they are placed in water. It's a rather foreseeable result, since HPMC is a hydrophilic polymer and SA is a hydrophobic acid. In practice, a clear solution is obtained by dispersing HPMC in water, whereas, a white colored solution is obtained for HPMC–SA mixture in water. As explained by Laboulfie [33], HPMC will generate a repulsive force on the surface of SA which will stabilize the mixture and prevent the agglomeration of SA particles, thus explaining the behavior that we sketched in Fig. 3.

The same conclusions are obtained for the couple HPMC–EC: HPMC will surround the hydrophobic particles of EC.

According to the tensile approach calculated using molecular simulation, there is no interactions between SA and PEG200 nor between EC and PEG200 (Table 19). On the other hand, the adhesion approach predicts that PEG200 will adhere over SA and over EC when placed in water which is in accordance with the fact that PEG200 is a hydrophilic polymer and SA and EC are both hydrophobic.

These conclusions lead to the suggestion that the work of adhesion approach may give better predictions than the tensile strength approach. Furthermore, the polarity of PEG400 is lower than that of PEG200, which means that PEG400 is less hydrophobic than PEG200. This was actually observed by Oelmeier [41] who stated that PEG with higher molecular weight have lower polarity and hence are less hydrophilic. This implies that, as we shift from PEG200 to PEG400, HPMC particles should surround PEG, and, as shown in Table 17, this is predicted by the work of adhesion approach. This was also observed experimentally by Laboulfie [33] for PEG1500. Additionally, the adhesion work approach predicts that PEG200 surrounds PEG400 which is in adequacy with the previous statements.

6. Conclusion

In this study, two approaches to predict the affinity between polymers and acid in binary mixture were analyzed and compared; the tensile strength approach and the work of adhesion approach. To extend the study to any compounds used in coating and granulation processes, the work of adhesion and the tensile strength formula were generalized with the inclusion of Hildebrand's solubility parameter. A correlation between surface free energy and solubility parameter for cellulose derivative was proposed. It yielded values for the work of cohesion in good agreement with those measured.

In the case of a ternary mixture, we derived an equation for the ideal tensile strength. This equation hints at which compound would predominantly surround the other in ternary mixtures.

The two models were applied to binary and ternary systems. The binary mixtures included a film forming polymer (HPMC), a hydrophobic filler (SA), a plasticizer (PEG), a binder/diluant (EC and MCC) and a

Table 18
Interactions predicted for NA and SA.

A	B							
	NA				SA			
	W_{ACB} CompassII	σ_{ACB} CompassII	W_{ACB} HSPiP	σ_{ACB} HSPiP	W_{ACB} CompassII	σ_{ACB} CompassII	W_{ACB} HSPiP	σ_{ACB} HSPiP
PVP	X	X	O	X	X	X	O	X
MCC	O	O	O	O	O	O	O	O
HPMC	M	M	M	O	O	O	O	O
EC	M	M	M	M	X	X	M	O
NA	–	–	–	–	M	X	O	X
SA	M	O	X	O	–	–	–	–
PEG200	M	M	O	M	O	M	O	M
PEG400	M	M	M	O	X	X	O	O

PVP: polyvinylpyrrolidone, MCC: microcrystalline cellulose, HPMC: hydroxypropyl-methylcellulose, EC: ethyl cellulose, NA: niflumic acid, SA: stearic acid, PEG: polyethylene glycol.
O: A surrounds B, X: B surrounds A, M: no interactions between A and B.

Table 19
Interactions predicted for PEG200 and PEG400.

A	B							
	PEG200				PEG400			
	W_{ACB} CompassII	σ_{ACB} CompassII	W_{ACB} HSPiP	σ_{ACB} HSPiP	W_{ACB} CompassII	σ_{ACB} CompassII	W_{ACB} HSPiP	σ_{ACB} HSPiP
PVP	X	X	M	X	M	X	M	O
MCC	O	O	O	O	O	O	O	O
HPMC	X	O	X	M	O	O	X	X
EC	X	M	X	M	M	M	X	X
NA	M	M	X	M	M	M	M	X
SA	X	M	X	M	O	O	X	X
PEG200	–	–	–	–	O	M	O	X
PEG400	X	M	X	O	–	–	–	–

PVP: polyvinylpyrrolidone, MCC: microcrystalline cellulose, HPMC: hydroxypropyl-methylcellulose, EC: ethyl cellulose, NA: niflumic acid, SA: stearic acid, PEG: polyethylene glycol.
O: A surrounds B, X: B surrounds A, M: no interactions between A and B.

pharmaceutical drug (NA). In ternary systems, water was added as a solvent to the previous mixtures. The two models gave similar results in good agreement with the available experimental observations overall, but the work of adhesion approach might give more accurate predictions than the ideal tensile strength approach. The prediction obtained using the work of adhesion confirmed the experimental observations of Laboulfie et al. [33]: SA particles are stabilized by HPMC particles in water. Also, the addition of PEG400 to the mixture holds the SA and HPMC particles together and consequently enhance the consistency of the formed hydrophobic film. The affinity between particles in aqueous systems is better when their interfacial nature is the opposite.

Appendix A. Work of adhesion equations

The full expressions of the work of adhesion given by Girifalco and Good [25] and Wu [26] are shown in the following table:

Table A.1
Work of adhesion equations proposed by Girifalco and Good [25] and Wu [26].

Girifalco and Good	Wu
$W_{AB} = 2\phi_I\phi_V(\gamma_A\gamma_B)^{0.5}$	$W_{AB} = 2\varphi_{AB}(\gamma_A\gamma_B)^{0.5}$
$\phi_I = \frac{\varepsilon_{AB}}{\varepsilon_A\varepsilon_B}$	$\varphi_{AB} = 2\left(\frac{x_A^d x_B^d}{g_A x_A^d + g_B x_B^d} + \frac{x_A^p x_B^p}{g_A x_A^p + g_B x_B^p}\right)$
$\phi_V = \frac{4(v_A v_B)^{1/3}}{(v_A^{1/3}+v_B^{1/3})^2}$	$x_i^p = \frac{\gamma_i^p}{\gamma_i}$ and $x_i^d = \frac{\gamma_i^d}{\gamma_i}$
	$g_A = \frac{\gamma_A}{\gamma_B}$ and $g_B = \frac{\gamma_B}{\gamma_A}$

Here, in Table A.1, in Girifalco and Good expression, the ε's are the repulsive potential constants, v_A and v_B the molar volumes of materials A and B respectively, γ_A and γ_B are the surface free energy of A and B respectively. For polymer molecules, it's better to interpret v as the molar volume of the polymer segment or the repeat unit [16].

In the expression of the work of adhesion proposed by Wu, x_i^p and x_i^d are the polar and the nonpolar fraction of phase i, and the ratios g_A and g_B are defined by the ratio of the surface free energy.

Appendix B. Surface free energy calculation using the molar parachor

The surface free energy is the thermodynamic work to be done per unit area of surface extension and as such is a manifestation of the intermolecular forces. Its value can be obtained indirectly from contact angle measurement of two liquids of known polarity or from empirical correlations to estimate the surface free energy. For polymers we have used the correlation with the molar parachor P [32]:

$$\gamma = \left(\frac{P}{v}\right)^4. \tag{B.1}$$

Here, γ is the surface free energy and v is the molar volume.

$$P = 3.989792\,V_W + N_{ps}0.502094 \tag{B.2}$$

where V_W is the Van der Waals volume and N_{ps} is a correction term:

$$N_{ps} = -3N_{(carbonatomswith\Omega=\Omega^v)} + 6N_{(carbonylsgroups)} + 16N_{(-S-)} + 6N_{Br} - 6N_F. \tag{B.3}$$

Here, $N_{(carbon\ atoms\ with\ \Omega = \Omega^v)}$ equals to the number of carbon atoms which are singly bonded to all of their neighbors, $N_{(carbonyl\ groups)}$ is the total number of carbonyl (–C═O), $N_{(-S-)}$, N_{Br} and N_F are the numbers of sulfur atoms in the lowest (divalent) oxidation state, bromine atoms, and fluorine atoms, respectively, in the repeat unit. For non-polymer compounds, we used the structural contribution method of Sugden found in Bicerano Book [32].

Appendix C. The ideal tensile strength in the third medium

In the general case of two different bodies A and B interacting in a third medium C, the relationship between the adhesive tensile strength and the work of adhesion is given by the following expression:

$$W_{ACB}(h) = \int_h^\infty \sigma(x)_{ACB}dx. \tag{C.1}$$

$W_{ACB}(h)$ is the work required to move to infinity the surface of a body A separated from another body B by a distance h and both placed in a third medium C, the previous equation can be converted to:

$$\sigma(x)_{ACB} = \frac{dW_{ACB}(h)}{dh}|_{h=\infty} - \frac{dW_{ACB}(h)}{dh}|_{h=x} = -\frac{dW_{ACB}(h)}{dh}|_{h=x}. \tag{C.2}$$

Then, using relationship (18), proposed by Israelachivili [36], we obtain the following equation:

$$\sigma(x)_{ACB} = -\frac{dW_{ACB}(h)}{dh}|_{h=x} = -\frac{dW_{AB}(h)}{dh}|_{h=x} - \frac{dW_{CC}(h)}{dh}|_{h=x} + \frac{dW_{AC}(h)}{dh}|_{h=x} + \frac{dW_{CB}(h)}{dh}|_{h=x}. \tag{C.3}$$

Now, let's follow the same route of resolution made by Gardon [27], he began by assuming a law of force between surfaces of particles instead of whole particles, then, he divided the surface of each particle into interacting sites. Under those assumptions, for two particles A and B in vacuum, he proposed the following equation of the tensile strength:

$$\sigma(x)_{AB} = -\frac{dW_{AB}(h)}{dh}|_{h=x} = \pi N_A N_B \left(\frac{\varepsilon_{AB}}{6x^3} - \frac{\lambda_{AB}}{90x^9}\right) \tag{C.4}$$

where ε_{AB} and λ_{AB} are the attractive and repulsive potential constants between A and B respectively, N_A and N_B are the number of sites interacting between A and B. Eq. (C.3) becomes:

$$\sigma(x)_{ACB} = \pi N_A N_B \left(\frac{\varepsilon_{AB}}{6x^3} - \frac{\lambda_{AB}}{90x^9}\right) \pi {N_C}^2 \left(\frac{\varepsilon_{CC}}{6x^3} - \frac{\lambda_{CC}}{90x^9}\right) - \pi N_C N_B \left(\frac{\varepsilon_{AC}}{6x^3} - \frac{\lambda_{AC}}{90x^9}\right) - \pi N_A N_C \left(\frac{\varepsilon_{BC}}{6x^3} - \frac{\lambda_{BC}}{90x^9}\right). \tag{C.5}$$

When two particles in a liquid are in equilibrium, $\sigma_{ACB} = 0$ and $x = d^0_{ACB}$:

$$d^0_{ACB} = \left(\frac{N_A N_B \lambda_{AB} + N_C^2 \lambda_{CC} - N_A N_C \lambda_{AC} - N_B N_C \lambda_{BC}}{15\left(N_A N_B \varepsilon_{AB} + N_C^2 \varepsilon_{CC} - N_A N_C \varepsilon_{AC} - N_B N_C \varepsilon_{BC}\right)}\right)^{(1/6)}. \tag{C.6}$$

This distance can be rewritten using the following relationships [27]:

$$\begin{aligned} W_{AB} &= 0.0625\pi N_A N_B \varepsilon_{AB} / {d^0_{AB}}^2 \\ d^0_{AB} &= \left(\frac{\lambda_{AB}}{15\varepsilon_{AB}}\right)^{1/6}. \end{aligned} \tag{C.7}$$

With d^0_{AB} is the distance where A and B in vacuum are in equilibrium and W_{AB} is the total adhesion work in binary mixture. Eq. (C.6) becomes:

$$d^0_{ACB} = \left(\frac{W_{AB}{d^0_{AB}}^8 + W_{CC}{d^0_{CC}}^8 - W_{AC}{d^0_{AC}}^8 - W_{BC}{d^0_{BC}}^8}{W_{AB}{d^0_{AB}}^2 + W_{CC}{d^0_{CC}}^2 - W_{AC}{d^0_{AC}}^2 - W_{BC}{d^0_{BC}}^2}\right)^{(1/6)}. \tag{C.8}$$

Using Eq. (6), d^0_{ACB} becomes:

$$d^0_{ACB} = \left(\frac{\sigma^{\max}_{AB}{d^0_{AB}}^9 + \sigma^{\max}_{CC}{d^0_{CC}}^9 - \sigma^{\max}_{AC}{d^0_{AC}}^9 - \sigma^{\max}_{BC}{d^0_{BC}}^9}{\sigma^{\max}_{AB}{d^0_{AB}}^3 + \sigma^{\max}_{CC}{d^0_{CC}}^3 - \sigma^{\max}_{AC}{d^0_{AC}}^3 - \sigma^{\max}_{BC}{d^0_{BC}}^3}\right)^{(1/6)}. \tag{C.9}$$

If the sites are in contact, spherical and identical, d^0_{AB} is the distance between the center of the neighboring sites of particle A and particle B. Henceforth, as Gardon suggested, we can write:

$$d^0_{AB} = \left(0.63\frac{6}{\pi N_{av}}\right)^{1/3} \frac{\left(v_A^{1/3} + v_B^{1/3}\right)}{2} = 0.629 \times 10^{-8}\left(v_A^{1/3} + v_B^{1/3}\right) \tag{C.10}$$

where v is the molar volume, N_{av} is the Avogadro number and 0.63 takes into account close random packing of the sites [42], Eq. (C.9) becomes:

$$d^0_{ACB} = 0.629 * 10^{-8}\left(\frac{\sigma^{\max}_{AB}\left(v_A^{1/3} + v_B^{1/3}\right)^9 + \sigma^{\max}_{CC}\left(2v_C^{1/3}\right)^9 - \sigma^{\max}_{AC}\left(v_A^{1/3} + v_C^{1/3}\right)^9 - \sigma^{\max}_{BC}\left(v_A^{1/3} + v_C^{1/3}\right)^9}{\sigma^{\max}_{AB}\left(v_A^{1/3} + v_B^{1/3}\right)^3 + \sigma^{\max}_{CC}\left(2v_C^{1/3}\right)^3 - \sigma^{\max}_{AC}\left(v_A^{1/3} + v_C^{1/3}\right)^3 - \sigma^{\max}_{BC}\left(v_B^{1/3} + v_C^{1/3}\right)^3}\right)^{(1/6)}. \tag{C.11}$$

Given that the sites are spherical, d^0_{ACB} should be equal or higher than d^0_{AB}.
By integrating the tensile strength $\sigma(x)_{ACB}$ in Eq. (C.5) from d^0_{ACB} to infinity, we obtain the total adhesive work in a medium C:

$$W_{ACB} = \frac{\pi N_A N_B \varepsilon_{AB} + \pi N_C^2 \varepsilon_{CC} + \pi N_A N_C \varepsilon_{AC} + \pi N_B N_C \varepsilon_{BC}}{16{d^0_{ACB}}^2}. \tag{C.12}$$

The maximum tensile strength $\sigma^{\max}_{ACB}$ between compounds A and B placed in a third medium is obtained by solving:

$$\frac{d\sigma(x)_{ACB}}{dx} = 0. \tag{C.13}$$

Thus, we obtain the distance $d_{ACB}^{\max}$ between A and B where the stress is maximum:

$$d_{ACB}^{\max} = \left(\frac{N_A N_B \lambda_{AB} + N_C^2 \lambda_{CC} - N_A N_C \lambda_{AC} - N_B N_C \lambda_{BC}}{5(N_A N_B \varepsilon_{AB} + N_C^2 \varepsilon_{CC} - N_A N_C \varepsilon_{AC} - N_B N_C \varepsilon_{BC})} \right)^{(1/6)} = 3^{(1/6)} d_{ACB}^{0}. \tag{C.14}$$

Hence, replacing x by $d_{ACB}^{\max}$ in Eq. (C.5) gives:

$$\sigma_{ACB}^{\max} = \frac{\pi N_A N_B \varepsilon_{AB} + \pi N_C \varepsilon_{CC} + \pi N_A N_C \varepsilon_{AC} + \pi N_B N_C \varepsilon_{BC}}{9 d_{ACB}^{\max 3}} = \frac{\pi N_A N_B \varepsilon_{AB} + \pi N_C \varepsilon_{CC} + \pi N_A N_C \varepsilon_{AC} + \pi N_B N_C \varepsilon_{BC}}{15.59 d_{ACB}^{0\ 3}}. \tag{C.15}$$

Substitution from Eq. (C.12), we obtain the relationship between the total work of adhesion and the ideal tensile strength:

$$\sigma_{ACB}^{\max} = \frac{1.0263 W_{ACB}}{d_{ACB}^{0}}. \tag{C.16}$$

An almost identical result can be obtained if, instead of using the Gardon's Eq. (6), we start with adhesive tensile strength formula based on Lennard–Jones law of force [43]:

$$\sigma_{AB}(x) = \frac{8 W_{AB}}{3 \upsilon_{AB}} \left(\left(\frac{\upsilon_{AB}}{x} \right)^3 - \left(\frac{\upsilon_{AB}}{x} \right)^9 \right). \tag{C.17}$$

If we envisage the atomic spacing υ_{AB} to be the potential equilibrium distance between A and B, after using the same previous method of computation, we will obtain:

$$\sigma_{AB}^{\max} = \frac{1.243 W_{AB}}{d_{AB}^{0}} \text{ and } \sigma_{ACB}^{\max} = \frac{1.243 W_{ACB}}{d_{ABC}^{0}}. \tag{C.18}$$

References

[1] L. Larry Augsburger, K. Murali, Theory of granulation, in: Dilip M. Parikh (Ed.), Handbook of Pharmaceutical Granulation Technology, 81, 1997, pp. 7–23.
[2] M. Hemati, M. Benali, in: Ulrich Bröckel, Willi Meier, Gerhard Wagner (Eds.), Product Design and Engineering: Best Practices, Vol. 1, 2007 (chapter 8, Weinheim).
[3] Per Holm high shear mixer granulators, in: Dilip M. Parikh (Ed.), Handbook of Pharmaceutical Granulation Technology, 81, 1997, pp. 151–204.
[4] J.D. Lister, B.J. Ennis, S.M. Iveson, K. Hapgood, Nucleation, growth and breakage phenomena in agitated wet granulation processes: a review, Powder Technol. 117 (2001) 3–39.
[5] B.J. Ennis, G.I. Tardos, R. Pfeffer, A microlevel-based characterization of granulation phenomena, Powder Technol. 65 (1991) 257–272.
[6] B.J. Ennis, G.I. Tardos, R. Pfeffer, The influence of viscosity on the strength of an axially strained pendular liquid bridge, Chem. Eng. Sci. 45 (1990) 3071–3088.
[7] M. Benali, V. Gerbaud, M. Hemati, Effect of operating conditions and physicochemical properties on the wet granulation kinetics in high shear mixer, Powder Technol. 190 (1–2) (2009) 160–169.
[8] R.I. Mahato, A.S. Narang, Pharmaceutical Dosage Forms and Drug Delivery, Second Edition CRC Press, 2011.
[9] S. Mattsson, Pharmaceutical binders and their function in directly compressed tabletsDissertation thesis Uppsala faculty of pharmacy, 2000.
[10] A. Jiménez, M.J. Fabra, P. Talens, A. Chiralt, Effect of lipid self-association on the microstructure and physical properties of hydroxypropyl-methylcellulose edible films containing fatty acids, Carbohydr. Polym. 82 (2010) 585–593.
[11] T.A. Iranloye, E.L. Parrott, Effects of compression force, particle size, and lubricants on dissolution rate, J. Pharm. Sci. 67 (1978) 535–539.
[12] R.C. Rowe, P.J. Sheskey, M.E. Quinn, Handbook of Pharmaceutical Excipients, 6th Edition Pharmaceutical Press, 2009.
[13] J. Kundu, C. Patra, S.C. Kundu, Design, fabrication and characterization of silk fibroin–HPMC–PEG blended films as vehicle for transmucosal delivery, Mater. Sci. Eng. C 28 (2008) 1376–1380.
[14] F. Laboulfie, Depôt en couche mince d'un multi-materiau à la surface de particules solides: application à l'enrobage de particules alimentaires, INPT, Toulouse, 2013.
[15] J.H. Hildebrand, The Solubility of Nonelectrolytes (New York), 1950.
[16] A.F.M. Barton, CRC Handbook of Solubility Parameters and Other Cohesion Parameters, 1991.
[17] G. Gee, Thermodynamic of Rubber Solutions and Gels in Advances in Colloid Science (New York), 1946.
[18] P. Choi, T. Kavassalis, A. Rudin, Measurement of three-dimensional solubility parameters of nonyl phenol ethoxylates using inverse gas chromatography, J. Colloid Interface Sci. 180 (1996) 1–8.
[19] C.M. Hansen, The three-dimensional solubility parameter — key to paint component affinities: I. Solvents, plasticizers, polymers, and resins, J. Coat. Technol. 39 (1967) 505–510.
[20] D.W. Van Krevelen, Chemical structure and properties of coal, XXVII-coal constitution and solvent extraction, Fuel (1965) 229–242.
[21] K.L. Hoy, New values of the solubility parameters from vapor pressure data, J. Coat. Technol 42 (1970) 76–118.
[22] P.A. Small, Some factors affecting the solubility of polymers, J. Appl. Chem. 3 (1953) 71–80.
[23] HSPiP V. 3.1 Software, http://www.hansen-solubility.com/HSPiP.html2010.
[24] M. Belmares, M. Blanco, W.A. Goddard III, R.B. Ross, G. Caldwell, S.H. Chou, J. Pham, P.M. Olofson, C. Thomas, Hildebrand and Hansen solubility parameters from molecular dynamics with applications to electronic nose polymer sensors, J. Comput. Chem. 25 (2004) 1814–1826.
[25] L.A. Girifalco, R.J. Good, A theory for the estimation of surface and interfacial energies. I. Derivation and application to interfacial tension, J. Phys. Chem. 61 (1957) 904–909.
[26] S. Wu, Polar and nonpolar interactions in adhesion, J. Adhes. 5 (1973) 39–55.
[27] J.L. Gardon, Variables and interpretation of some destructives cohesion and adhesion tests, Treatise on Adhesion and Adhesives1967. 269–324.
[28] J.L. Gardon, Critical review of concepts common to cohesive energy surface tension, tensile strength, heat of mixing, interracial tension, and butt joint strength, J. Colloid Interface Sci. (1977) 582–596.
[29] R.C. Rowe, Adhesion of film coating to tablet surfaces — a theoretical approach based on solubility parameters, Int. J. Pharm. (1988) 219–222.
[30] J. Barra, F. Lescure, F. Falson-Rieg, E. Doelker, Can the organization of a binary mix be predicted from the surface energy, cohesion parameter and particle size of its components? Pharm. Res. 15 (1998) 1727–1736.
[31] M. Benali, Prédiction des interactions substrat-liant lors de la granulation: Etude expérimentale dans un mélangeur à fort taux de cisaillement, approches thermodynamiques par simulation moléculaire, 2006.
[32] J. Bicerano, Prediction of Polymer Properties, CRC Press, 2002.
[33] F. Laboulfie, M. Hemati, A. Lamure, S. Diguet, Effect of the plasticizer on permeability, mechanical resistance and thermal behaviour of composite coating films, Powder Technol. 238 (2013) 14–19.
[34] Accelrys Material Studio Suite release 7, http://accelrys.com/products/materials-studio2013.
[35] H. Flyvbjerg, H.G. Petersen, Error estimates on averages of correlated data, J. Chem. Phys. 91 (1989) 461–467.
[36] J.N. Israelachvili, Intermolecular and Surface Forces, Academic Press, 2010.
[37] D. Frenkel, B. Smit, Understanding Molecular Simulation, Academic Press, 1996.
[38] R. Bonn, J.J. van Aartsen, Solubility of polymers in relation to surface tension and index of refraction, Eur. Polym. J. 8 (1972) 1055–1066.
[39] T.J. Sheldon, C.S. Adjiman, J.L. Cordiner, Pure component properties from group contribution: hydrogen-bond basicity, hydrogen-bond acidity, Hildebrand solubility parameter, macroscopic surface tension, dipole moment, refractive index and dielectric constant, Fluid Phase Equilib. 231 (2005) 27–37.
[40] Z. Lovorka, B. Graham, The use of surface energy values to predict optimum binder selection for granulations, Int. J. Pharm. 59 (1990) 155–164.
[41] S.A. Oelmeier, F. Dismer, J. Hubbuch, Molecular dynamics simulations on aqueous two-phase systems — single PEG-molecules in solution, BMC Biophys. 5 (2012) 14.
[42] G.D. Scott, Nature 199 (1960) 908.
[43] J.A. Greenwood, Adhesion of elastic spheres, Math. Phys. Eng. Sci. 453 (1961) (2001) 1277–1297.
[44] J.E. Mark, Polymer Data Handbook, 1998.
[45] J. Barra, F. Falson-Rieg, E. Doelker, Influence of the organization of binary mixes on their compactibility, Pharm. Res. 16 (1999) 1449–1455.

[46] M. Ash, I. Ash, Handbook of Green Chemicals, 1998.
[47] R.C. Rowe, Interactions in coloured powders and tablet formulations: a theoretical approach based on solubility parameters, Int. J. Pharm. 53 (1989) 47–51.
[48] L.P. Demajo, D.S. Rimai, L.H. Sharpe, Fundamentals of Adhesion and Interfaces, CRC Press, 2000.
[49] R.C. Rowe, Polar/non-polar interactions in the granulation of organic substrates with polymer binding agents, Int. J. Pharm. 56 (1989) 117–124.
[50] P. Bustamante, A. Martin, M.A. Gonzalez-Guisandez, Partial solubility parameters and solvatochromic parameters for predicting the solubility of single and multiple drugs in individual solvents, J. Pharm. Sci. 82 (1993) 635–640.
[51] A. Onions, Films from water-based colloidal dispersions, Manuf. Chem. 12 (1986) 55–59.

Ahmed Jarray is a Ph.D. student at the Institut National Polytechnique de Toulouse (INPT). He has an Ing. in Chemical and Process Engineering (2011, Gabes, Tunisia) and a MSc in Process Engineering (2012, Lyon, France).

Vincent Gerbaud is a research manager at The Centre National de la Recherche Scientifique (CNRS). He has a BSc in Chemical Engineering (1991, Toulouse, France), MSc in Chemical Engineering (1992, UMASS, USA) and a PhD in Chemical Engineering (1996, Toulouse, France). He conducts research in process system engineering, with a strong interest in small scale modeling: molecular simulation, thermodynamics, computer aided molecular and mixture design, He has supervised 12 PhD thesis and 11 post-docs (for more details please visit: http://lgc.inp-toulouse.fr/lgc/annuaire/cv/vincent-gerbaud.pdf).

Mehrdji Hemati is a professor at the Institut National Polytechnique de Toulouse (INPT) since 1994, and animator of the team "Fluidization for Energy, CVD and new materials", He has 33 PhD theses supervised at INPT, and author or co-author of more than 100 publications in International Scientific Journals and 15 patterns.